Research article

Journal of RAMAN SPECTROSCOPY

Received: 7 July 2016 Revised: 20 December 2016 Accepted: 22 December 2016 Published online in Wiley Online Library: 7 April 2017

(wileyonlinelibrary.com) DOI 10.1002/jrs.5101

Label-free surface-enhanced Raman spectroscopy of lipid-rafts from hepatocyte plasma membranes

Blanca Delgado-Coello,[a†] Danai Montalvan-Sorrosa,[a,d†] Armando Cruz-Rangel,[a] Marcela Sosa-Garrocho,[b] Beatriz Hernández-Téllez,[c] Marina Macías-Silva,[b] Rolando Castillo[d] and Jaime Mas-Oliva[a]*

Lipid rafts are sphingomyelin/cholesterol-rich domains present in the plasma membrane of eukaryotic cells. In the hepatocyte, it has been shown that these domains intervene and modify a wide range of functions from which cell signaling in health and disease is of major importance. The present investigation proposes a novel strategy for the study of plasma membrane lipid rafts using surface-enhanced Raman spectroscopy (SERS) and spectra processing employing the principal component analysis (PCA) in correlation with conventional biochemical techniques. SERS has been used for artificial membranes; our approach has the advantage that allows studying purified biological membranes using small volumes of biological samples and a very simple protocol. Therefore, the use of SERS/PCA represents an important advantage for the study not only of the structure and composition of biological membranes but also for the understanding of the functions carried by the membrane-embedded proteins. Our work using SERS/PCA for the first time shows a correlation when studying the composition of lipid rafts from the cell plasma membrane and the catalytic activity of the Ca^{2+}-ATPase, and its direct association with the presence of specific lipids located in membrane lipid rafts. Also, we show that changes in plasma membrane and the catalytic activity of the Ca^{2+}-ATPase activity present in the plasma membrane of hepatocytes after partial depletion of membrane cholesterol carried out by methyl-beta-cyclodextrin correlate with the changes in the enzyme activity and the presence of cholesterol-rich domains of lipid rafts. Copyright © 2017 John Wiley & Sons, Ltd.

Keywords: SERS; PCA; hepatocyte; plasma membrane; lipid rafts; cholesterol

Introduction

Cholesterol is one of the most important lipids in the plasma membrane of eukaryote cells; it can be organized following a free distribution, or as part of microdomains named lipid rafts.[1–5] Rafts are sphingomyelin/cholesterol-rich domains of sizes ranging between 10 and 200 nm; they provide highly ordered localized molecular arrangements in which proteins move laterally across the plain of cell membranes.

It is widely accepted that lipid rafts play a role in protein/lipid sorting and signaling processes in the eukaryotic cell; they are considered dynamic domains that can be organized in very short times (nanoseconds), property that contributes to the skepticism regarding its true presence in the membrane. Several microscopy techniques have been used to study lipid rafts or detergent-resistant membranes (DRM); among others, confocal microscopy, total internal fluorescent microscopy,[6] and fluorescence lifetime imaging microscopy combined with Förster resonance energy transfer.[7] In recent years, the use of Raman spectroscopy for the analysis of biomolecules has been proposed as an attractive alternative to traditional methods as this technique is non-destructive, non-invasive, and it requires minimal amounts of sample and involves simple preparation steps. For example, work using Raman microscopy employing synthetic monolayers with a lipid content similar to that characteristic of rafts[8] or including sphingolipids specifically modified for their use as Raman probes has been reported.[9] An interesting investigation exploring segments of the thoracic aorta from db/db mice (experimental model for type 2 diabetes) using tip-enhanced Raman spectroscopy and atomic force microscopy confirmed the presence of several types of lipid rafts and also their clustering in comparison with samples obtained from db + heterozygotic mice.[10]

* *Correspondence to: Jaime Mas-Oliva, Departamento de Bioquímica y Biología Estructural, Instituto de Fisiología Celular, Universidad Nacional Autónoma de México, Apartado Postal 70-243, C.P. 04510, Mexico City, Mexico. E-mail: jmas@ifc.unam.mx*

† *These authors contributed equally to this work.*

a *Departamento de Bioquímica y Biología Estructural, Instituto de Fisiología Celular, Universidad Nacional Autónoma de México, Mexico City, Mexico*

b *Departamento de Biología Celular y del Desarrollo, Instituto de Fisiología Celular, Universidad Nacional Autónoma de México, Mexico City, Mexico*

c *Departamento de Biología Celular y Tisular, Facultad de Medicina, Universidad Nacional Autónoma de México, Mexico City, Mexico*

d *Instituto de Física, Universidad Nacional Autónoma de México, Mexico City, Mexico*

In the hepatocyte, the presence and relevance of cholesterol-rich domains during normal and pathological conditions has been previously reviewed.[11,12] Cholesterol not only serves as a structural component of membranes but also appears to modulate the activity of several membrane proteins in both, the quiescent and the proliferating liver.[13] Therefore, the aim of the present study is to show the usefulness of surface-enhanced Raman spectroscopy (SERS) in the identification and characterization of DRM obtained from the hepatocyte plasma membrane when it is used in conjunction with the principal component analysis (PCA). As part of the characterization of DRM, our investigation shows the plasma membrane and the catalytic activity of the Ca^{2+}-ATPase (PMCA) as the catalytic representation of the calcium pump in direct association with these domains and the strict correlation of changes in enzymatic activity modulated by cholesterol. Moreover, the expression of housekeeping transcripts of PMCA in cultured hepatocytes where cholesterol was partially depleted was also studied.

Materials and methods

Experimental animals

Male Wistar rats (mean weight, 250 g) were handled and sacrificed following the Mexican Official Norm for Laboratory Animals (NOM-062-ZOO-1999) and an experimental protocol approved by the Animal Care and Use Committee of our institution (JMO61–15).

Isolation of detergent-resistant membranes

Crude plasma membranes were isolated from fresh exsanguinated livers obtained from two rats in Krebs-Ringer solution as previously reported.[14] Briefly, each membrane pellet was resuspended in 10 mM Tris–HCl (pH 7.4), slightly homogenized and stored at −70 °C until further use. For each isolation of DRM (three different preparations), crude membrane samples obtained from two complete livers were centrifuged at 31 000 *g* for 10 min, and pellets solubilized for 1 h with 1% Triton X-100 at 4 °C in a buffer containing 50 mM Tris–HCl, 25 mM KCl, 5 mM $MgCl_2$, and 1 mM EDTA (pH 8.0). Solubilized membranes were recovered after centrifugation at 15 000 *g* for 10 min, and their density adjusted to 40% with sucrose in a refractometer (Carl Zeiss; Oberkochen, Germany). Two additional layers of 38% sucrose and 5% sucrose prepared in solubilization buffer without detergent were subsequently added (4 ml each) and centrifuged at 135 000 *g* at 4 °C for 21 h in a Beckman SW40 rotor. Twelve fractions of 1 ml of volume were collected, starting from the top of the gradient (labeled F1 to F12) downwards. Protein concentrations were determined using the Micro BCA Protein Assay Kit (Pierce; Rockford, IL, USA). Membrane cholesterol content was determined using the Amplex Red Cholesterol kit (Invitrogen; Eugene, OR, USA) in a Synergy HT Microplate Reader (Biotek Instruments, Inc., Winooski, VT, USA) at wavelengths of 530/590 nm (excitation/emission). Ca^{2+}-ATPase activity was determined at 37 °C using 25 μg of membrane protein in a reaction mixture containing 1.36 mM $MgCl_2$, 20 mM MOPS (pH 7.4), 260 mM KCl, 6.7 mM ATP, 1 mM EGTA, and a final free Ca^{2+} concentration of 10 μM. Released Pi was measured according to the method described by Lanzetta *et al.*[15] and expressed as specific activity (nmoles Pi mg^{-1} min^{-1}). Enzymatic activity was also measured in independent plasma membrane preparations in the presence of methyl-*β*-cyclodextrin [M*β*CD; Sigma-Aldrich (St. Louis MO, USA)].

Western blot assays

Fifty micrograms of total protein obtained from gradient fractions were separated on SDS-polyacrylamide gels and transferred onto nitrocellulose membranes (Bio-Rad; Hercules, CA, USA). Membranes were blocked overnight at 4 °C with a buffer containing 20 mM Tris–HCl (pH 7.5), 150 mM NaCl, 0.05% Tween-20, and 2.5% fat-free milk (milk-TBST). Membranes were incubated 1 h at 37 °C with a monoclonal flotillin-2 (or reggie-1) antibody (sc- 28320, Santa Cruz Biotechnology; Santa Cruz, CA, USA) diluted 1:1000 in milk-TBST. Also, blots were incubated with a monoclonal PMCA antibody (MA3–914, Thermo Fisher Scientific Inc., Rockford IL, USA) diluted 1:2000 (clone 5F10). Membranes were washed three times with TBST and incubated with the corresponding secondary antibodies (1:5000) for 1 h at room temperature (RT). Membranes were washed three times with TBST, and the immunoreactive bands present detected with the Immobilon chemiluminescent HRP reagent (Merck Millipore; Billerica, MA, USA).

Gold nanoparticles synthesis

Synthesis of gold nanoparticles (AuNPs) was performed as reported elsewhere[16] and achieved by mixing 30 ml of a solution of gold hydrochloride (Sigma-Aldrich) with the same volume of a preheated sodium citrate (Sigma-Aldrich) solution used as reducing agent, employing gentle stirring and a temperature of 100 °C. Both solutions were used at the same concentration (0.5 mM) and prepared with ultrapure water. When the color for this mixture changed from pale yellow to bright pink (around 30 min), the synthesis of 30 nm AuNPs was completed. The suspension was immediately used to prepare samples for SERS. Sizes and shapes of AuNPs were confirmed by transmission electron microscopy.

Surface-enhanced Raman spectroscopy

Surface-enhanced Raman spectroscopy spectra from the sucrose gradient fractions (F5 to F12) were obtained with a DXR Raman microscope (Thermo Scientific; Madison, WI, USA) using a diode-pumped solid-state 532-nm laser. For SERS, samples were prepared by adding freshly prepared 30 nm AuNPs to each fraction (3:1 *v*/v). Mixtures were vigorously agitated and maintained at RT for 12–24 h.[16] A drop of sample (10 μl) was placed in a CaF_2 slide and spectra collected as fast as possible to avoid drop evaporation. For each sample, at least 15 SERS spectra within the 700–2500 cm^{-1} range were collected employing 15 exposures of 10 s each without fluorescence correction.

The PCA was performed using a MatLab algorithm by which the first three principal components were obtained. For this procedure, matrices were constructed; columns and rows corresponded to the measured intensity of spectra and the specific Raman wavenumbers, respectively. Raw spectra processing involved performing baseline correction, smoothing, and normalization to remove noise.

PMCA transcripts quantitation on cultured hepatocytes exposed to M*β*CD

Primary cultures of hepatocytes were obtained as previously described and used 1 day after being plated in dishes coated with collagen type I.[17] Cell viability was assayed using a 3-(4–5-dimethylthiazol-2-yl)-2,5-diphenyl tetrazolium (MTT) reduction assay (Sigma-Aldrich). Briefly, hepatocytes (7.5×10^4 cells/well)

Journal of RAMAN SPECTROSCOPY

in 12-well dishes were treated in triplicate with MβCD in DMEM medium (Invitrogen; Carlsbad, CA) at 37 °C for 24 h. Afterwards, the medium was changed, and cells incubated at 37 °C with a 0.5 mg/ml MTT solution for 2 h. The MTT formazan crystals were solubilized with 500 μl of DMSO for 30 min at RT and absorbance measured at 595 nm using a Biotek ELx800 microplate reader.

In parallel experiments, primary cultured hepatocytes were exposed to MβCD (0.5–1.0 mM) for 24 h. After removing the reagent, cells were scraped from the plates with Trizol reagent, frozen in liquid nitrogen, and stored at −70 °C. Taqman probes for the housekeeping *PMCA* isoforms, *PMCA1* and *PMCA4* (Primer Design Ltd, Southampton, UK) [17], were combined with 0.5 μg total RNA (treated with DNAse I) in a final volume of 20 μl using the CellsDirect kit (Invitrogen, Carlsbad, CA) and the StepOnePlus System (Applied Biosystems; Life Technologies). The amplification cycles included as follows: 50 °C for 15 min, 95 °C for 2 min, and 40 cycles of 95 °C for 15 s and 60 °C for 30 s. Statistical analyses were performed using the Prism de GraphPad Software V6.0; and values for $P < 0.05$ were considered significant.

Results and discussion

Biochemical analysis of lipid rafts from hepatocyte membranes

Cholesterol is abundant in the plasma membranes of hepatocytes showing a differential distribution in the canalicular domain where its concentration is twice of that in the basolateral domain.[18–20] Also, cholesterol has been shown to be present in lipid rafts domains of parenchymal (hepatocytes) and non-parenchymal cells (including Kupffer cells, sinusoidal endothelial cells, and hepatic stellate cells) showing an important role in the establishment of calcium waves between hepatocytes.[11,12,21]

As a first approach, we performed the biochemical analysis of fractions collected from the sucrose gradients and found that total protein and cholesterol are enriched in fraction 5 associated with a light layer (density of 28%), indicating that this fraction corresponds to DRM (Fig. 1(a) and (b)). Hepatocyte-derived DRM obtained in the present study exhibit a protein/cholesterol profile similar to that observed for DRM isolated from other tissues.[14,20,22] Gradient fractions were further characterized by Western blot analysis using antibodies recognizing flotillin-2 (or reggie-1) considered a marker for raft domains in several mammalian species (Fig. 1(d)).[23]

Because our group has been interested in understanding the relationship between the specific distribution of the several PMCA isoforms expressed in the hepatocyte and their function within the regulation of the homeostasis of calcium within the cell,[17,24,25] we measured Ca^{2+}-ATPase activity in the gradient fractions (Fig. 1(c)) in parallel with identification of the housekeeping isoforms of this enzyme (PMCA1 and PMCA4) by Western blot analysis (Fig. 1(e)).[26] So as to attempt the identification of markers, we concentrated fractions F1–F4; only fraction 4 had enough protein concentration to be loaded on an sodium dodecyl sulfate polyacrylamide gel electrophoresis gel, and therefore, the only one included in the Western blot assays together with fractions F5–F12. Positive bands for flotillin-2 and PMCA proteins were detected only in fractions 5–9 with an apparently higher content in fraction 5 (Fig. 1(d) and (e)). DRM identity was confirmed by the presence of flotillin-2, and also by the presence of the most abundant constitutive isoform of PMCA in liver tissue.[24,27]

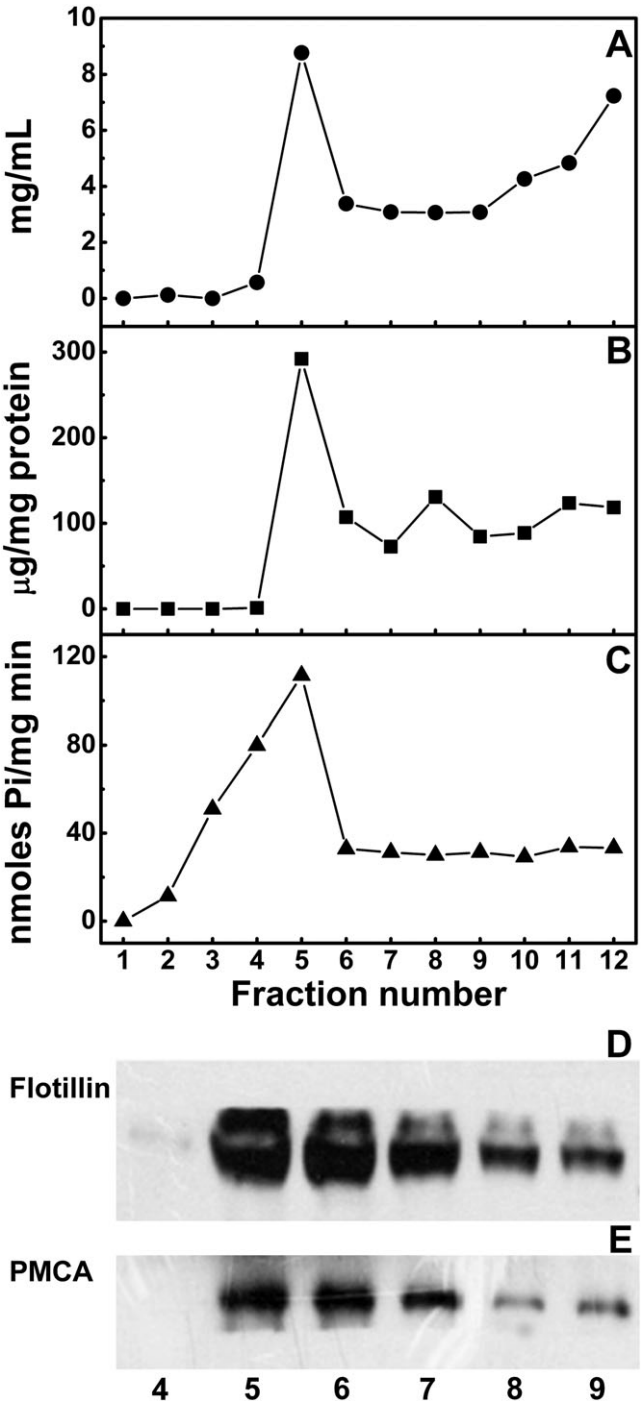

Figure 1. Representative analysis of fractions obtained from liver membranes solubilized with 1% Triton X-100 and fractionated using a sucrose density gradient: (a) Protein profile (●); (b) cholesterol profile (■); (c) specific Ca^{2+}-ATPase activity (▲) (note that fractions 1–4 were concentrated to measure ATPase activity). (d) Immunoblot detection of flotillin-2 and (e) total plasma membrane calcium ATPase (PMCA) found in sucrose gradient fractions 5–9. Note that fraction 4 previously concentrated was also included in this assay.

Surface-enhanced Raman spectroscopy of lipid rafts

Sample preparation for SERS only requires the addition of noble metal nanoparticles (AuNP's) to the different fractions to obtain enhanced signals by several orders of magnitude.[16,28] Taking advantage of the potential of SERS for membrane studies and the

characterization of bionanocomposites, [16] we used this methodology to analyze the sphingomyelin/cholesterol-rich domains of the plasma membrane fractions isolated from liver cells (fractions F5–F12). We employed this method in conjunction with PCA because the very small volumes of sample needed and no requirements for labeling. This technique can be used as a routine analytical tool when studying molecular changes associated with specific compartments of the cell because it is a non-destructive method and sample analysis can be carried out in aqueous suspensions.

Figure 2 shows the average SERS spectra of eight of the collected fractions (F5–12). Functional groups common to all spectra between wavelengths 700 and 2500 cm^{-1} were assigned and summarized in Table 1. As expected, these gradient fractions share vibrational modes related to proteins and lipids associated with the DRM from hepatocyte membranes. The most evident differences among spectra appear between 1600 and 2500 cm^{-1}. Nucleic acids derived from contaminant genomic material present in the samples were also detected (peaks between 2300 and 2400 cm^{-1}, pyridines and pyrimidines around 968 cm^{-1}), as well as remnant polysaccharides from sucrose used to prepare gradients (primary and secondary alcohols located around 830 cm^{-1} and aldehydes around 1370 cm^{-1}).

The main differences among the collected sucrose gradient fractions were determined by applying PCA to a matrix made of SERS spectra. This statistical procedure reduces complex spectra data sets to lower data dimensions with minimal loss of information. PCA also facilitates the identification of patterns in data sets, thereby highlighting major differences. All collected spectra from fractions F5 to F12 were used for the analysis, taking into account that F5 contains most of the DRM. Figure 3(a) shows a tridimensional plot of the three first principal components for the eight fractions that apparently cluster in three principal groups, one including spectra from F7 and F8, a second one formed by fractions F5, F6, F9, and F10; and a third group including the spectra from fractions F11 and F12. So as to show that these main clustering groups contain well separated fractions, we further analyzed spectra corresponding to F9 and F10, F5, and F6 (Fig. 3(b)). However, a separate PCA analysis shows that both pairs F5 and F6 (Fig. 3(c)) and F11 and F12 (Fig. 3(d)) present important differences between them. Interestingly, because F5 and F6 correspond to consecutive fractions, they also share common membrane proteins as shown before in the immunoblot assays (Fig. 1(d) and (e)). Therefore, it is not unexpected that they appear as if they were a group (Fig. 3(a) and (b)). Differences found in the tridimensional plot can be associated with the different variety of molecules existing in each fraction. To identify the corresponding functional groups, we use PCA to analyze differences between two well-separated fractions, F5 and F10. In this respect, because F5 corresponds to an enriched DRM fraction while F10 presents no DRM, Fig. 4 shows Raman wavenumber *versus* the first principal component, where the highest peaks indicate the main differences between the analyzed spectra. Functional groups were assigned and summarized in Table 2. The

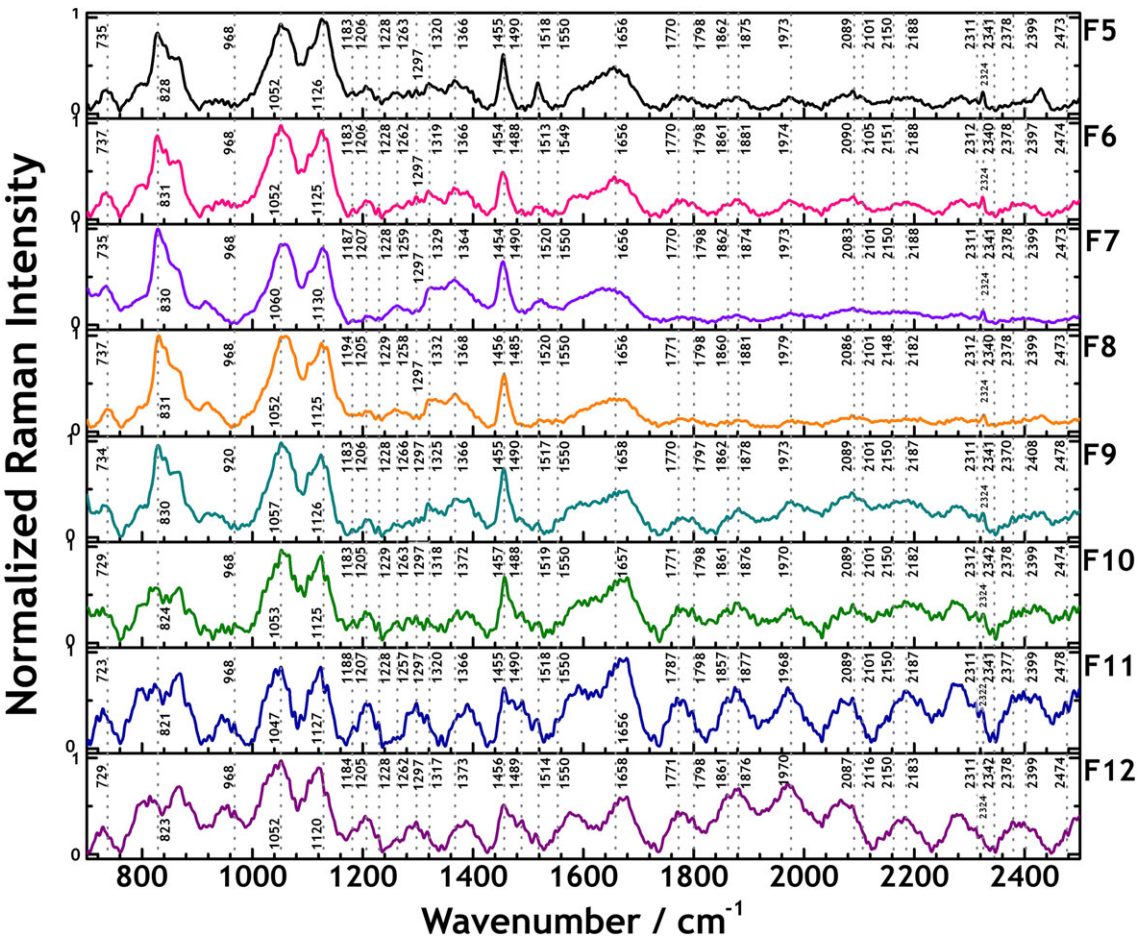

Figure 2. Surface-enhanced Raman spectroscopy of liver plasma membranes fractions obtained from sucrose gradients. Average surface-enhanced Raman spectroscopy of at least 15 spectra for each fraction collected is shown. Dotted lines indicate the common peaks found in the comparison among fractions spectra. Representative data of one detergent-resistant-membrane preparation.

Table 1. Common functional groups obtained from sucrose gradient fractions

Raman wavenumber (cm^{-1})								Vibrational mode	Tentative functional groups assignment
F5	F6	F7	F8	F9	F10	F11	F12		
735	735	735	737	734	729	723	729	s, p asym CNC str	Tertiary amides
								m-s, ring vib	Para disubstituted benzenes
								m-s, p asym CSC str	CH_3SCH_2-
								m-s, sym skeletal vib	Tertiary butyl groups
								s, C–S str	Aliphatic sulphides and disulphides
828	828	830	831	830	824	821	823	m-s, skeletal vib	Straight chain and branched alkanes
								s, p O–O str	Primary and secondary alcohols
								s, p asym CNC str	Tertiary amides
								s, POP str	P-O-P
968	967	968	968	920	968	968	968	s, p sym COC str	Ethers
								vs ring vib	Polysubstituted pyridines
								m-s C=C, C=N str	Pyrimidines
								m CH def	*trans* CH = CCH– and *cis* CH = CH–
1052	1052	1060	1052	1057	1053	1047	1052	s, p sym COC str	Ethers
								m-s CCC str	Straight chain alkanes
								m-s ring vib	2-Monosubstituted pyridines
1126	1125	1130	1125	1126	1125	1127	1120	m-s C–N str	Aliphatic amines
								s, p sym COC str	Ethers
1183	1183	1187	1194	1183	1183	1188	1184	m-s C–N str	Aliphatic amines
1206	1206	1207	1205	1206	1205	1207	1205	*s* CH def	*cis* (sat) CH = CH (sat)
								m-s C–N str	Aliphatic amines
								m-s, C–O–C str	Formates
1228	1228	1228	1229	1228	1229	1228	1228	s CH def	*cis* (sat) CH = CH (sat)
								m-s CO–O str	Acetates
								m-s C–N str	Aliphatic amines
1263	1262	1259	1258	1266	1263	1257	1262	s CH def	*cis* (sat) CH = CH (sat)
1297	1297	1297	1297	1297	1297	1297	1297	s CH def	*trans* (sat) CH = CH (sat)
								s amide III	*trans*-secondary amides
1320	1319	1329	1332	1325	1318	1320	1317	s-m asym N–C–N str	Ureas
								s C–N amide III	Secondary amides
								s CH def	*trans* (sat) CH = CH (sat)
								s amide III	–CO NH CH_3
1366	1366	1364	1368	1366	1372	1366	1373	m-s, p sym CO_2- str	Carboxylate ions (aq. sln.)
								m-s, p CH_2 def	Vinyls –CH = CH_2
								s-m, CH in-plane rocking	Aldehydes and aryl aldehydes
1455	1454	1454	1456	1455	1457	1455	1456	m-w, OCH_3 OCH_2 def	–OCH_3OCH_2–
								m-w, OCH_3 CH_2 def	n-Alkanes and cyclopropyl compound
1490	1488	1490	1485	1490	1488	1490	1489	m-w, OCH_3 OCH_2 def	–OCH_3OCH_2–
1518	1513	1520	1520	1517	1519	1518	1514	w, NH def	Secondary amines
								w, sym NH_3^+ def	–NH_3^+
1550	1549	1550	1550	1550	1550	1550	1550	w, asym $CO^-{}_2$ str	Carboxylic acid salts –CO_2^-
								w, NH def	Secondary amines
1656	1656	1656	1656	1658	1657	1656	1658	*m-s,* C=N str	Imines >C=N–
								s, p C=C str	*cis* CH = CH–
1770	1770	1770	1771	1770	1771	1787	1771	m, p C=O str	Aryl and a,b-unsat acid chlorides
1798	1798	1798	1798	1797	1798	1798	1798	m-w, p C=O str	Sat. aliphatic acid chlorides
1862	1861	1862	1860	1862	1861	1857	1861	m-w, sym C=O str	Sat. 5 membered ring cyclic anhydrides
1973	1974	1973	1979	1973	1970	1968	1970	v, asym C=C=C str	Allenes
2089	2090	2083	2086	2089	2089	2089	2087	m-s, p br asym NCS str	Isothiocyanates –N=C=S
2101	2105	2101	2101	2101	2101	2101	2116	v, asym -N=C=C str	ketenimines >C=N=N– and ketenes >C=C=O
2150	2151	2150	2148	2150	2150	2150	2150	v, asym -N=C=C str	ketenimines >C=N=N– and ketenes >C=C=O
								s, C=C str	Alkyl alkynes
2188	2188	2188	2182	2187	2182	2187	2183	v, asym -N=C=C str	Ketenimines >C=N=N– and ketenes >C=C=O
2311	2312	2311	2312	2311	2312	2311	2311	m-w, P-H str	P–H
2324	2324	2324	2326	2324	2325	2322	2321	m-w, P-H str	P–H

(Continues)

Table 1. *(Continued)*

Raman wavenumber (cm^{-1})								Vibrational mode	Tentative functional groups assignment
F5	F6	F7	F8	F9	F10	F11	F12		
2341	2340	2341	2340	2341	2342	2341	2342	m-w, P-H str	P–H
2378	2378	2378	2378	2370	2378	2377	2378	m-w, P-H str	P–H
2399	2397	2399	2399	2408	2389	2399	2390	m-w, P-H str	P–H
2473	2474	2473	2473	2478	2474	2478	2474	m-w, P-H str	P–H

s, strong; p, polarized; asym, asymmetric; str, stretching; m, medium; vib, vibration; sym, symmetric; vs, very strong; def, deformation; sat, saturated; aq. sln., aqueous solution; unsat, unsaturated; w, weak; v, variable.

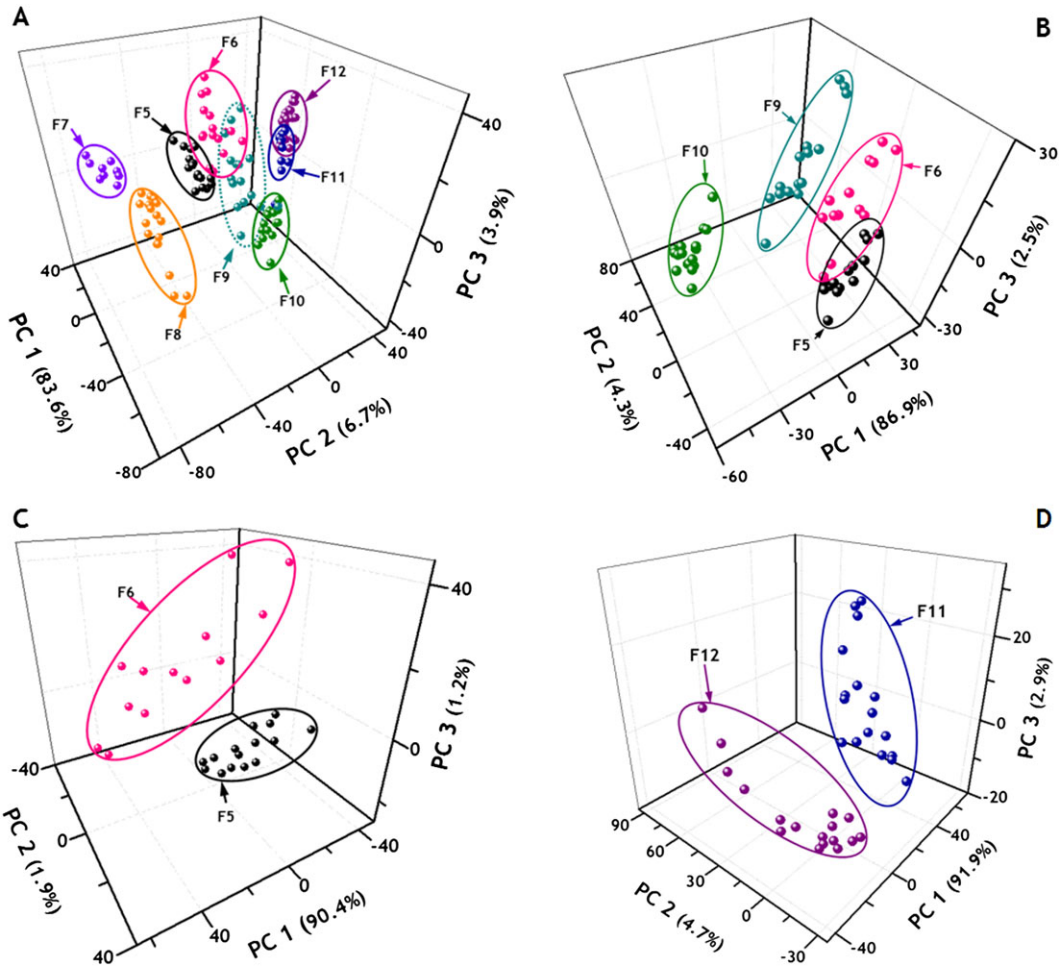

Figure 3. Three-dimensional plot of the first three largest principal components obtained from surface-enhanced Raman spectroscopy spectra of fractions shown in Fig. 2; their percentage contribution to the total variance is shown in parenthesis. Principal component analysis from fractions (a) F5 to F12; (b) F5, F6, F9, and F10; (c) F5 and F6; (d) F11 and F12. Total explained variance by PCs corresponds to the following: (a) 94.2%; (b) 93.7%; (c) 93.5%; (d) 99.5%.

main differences between F5 and F10 are located in 893, 1095, 1276, 1293, 1315, and 1434 cm^{-1}, mostly related to C–C bond vibrations from lipids,[29–31], in agreement with results obtained by the specific measurement of cholesterol and the presence of flotillin-2 (Fig. 1(d)). Signals at 1434 and 1675 cm^{-1} are related to the presence of cholesterol, fatty acids, and cholesterol esters, respectively,[30] suggesting that one of the analyzed samples is rich in cholesterol, as shown earlier that was F5. According to Talari *et al.*, peaks corresponding to 1095 and in 1545 cm^{-1} are related to lipids and six-membered rings present in cholesterol.[32]

Even though SERS from all fractions are relatively identical, by PCA, we concluded that isolated fractions were biochemically different, clearly evident for fraction F5 corresponding to the richest in protein and cholesterol content. A similar approach to the one we presented here has been reported for the study of bovine corneas using SERS with silver AuNPs.[33] Different lipids and proteins were identified, corresponding to molecules from the plasma membrane such as cholesterol and fatty acids.

To find out the characteristic peaks from lipid rafts, we compared SERS spectra from fractions F5, F8, F10, and F12 by PCA. Figure S1

Journal of RAMAN SPECTROSCOPY

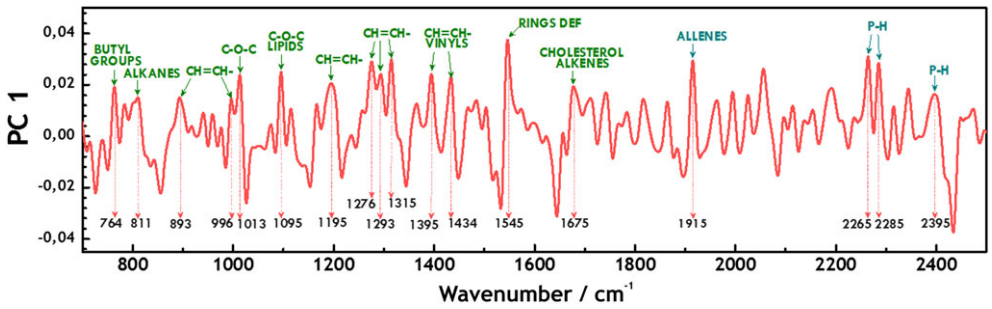

Figure 4. Main spectra differences PC 1 values given by principal component analysis *versus* the Raman wavenumber for F5 and F10 surface-enhanced Raman spectroscopy spectra. Highest peaks indicate main differences between compared spectra; the functional groups related with lipids are shown in green.

Table 2. Principal differences between fractions F5 and F10 obtained with principal component analysis

Raman wavenumber (cm^{-1})	Type of mode	Tentative functional groups
764	m, p skeletal vib	Branched alkanes
	m-s, p asym CSC str	CH_3SCH_2–
	m-s sym skeletal vib	Tertiary butyl groups
—	**Pyrimidine ring breathing mode**	—
811	m-s, skeletal vib	Straight chain alkanes
	s, p O–O str	Primary and secondary alcohols
	s, p asym CNC str	Tertiary amides
	s, POP str	P–O–P **from RNA**
	s, P=S str	P=S
	m, p skeletal vib	Branched alkanes
893	m, CH def	*cis* CH=CH–
	m-s, skeletal vib	Straight chain alkanes
	s, p O–O str	Primary and secondary alcohols
996	s, ring vib	Pyridines
	m-s, p ring vib	Cyclobutanes and cyclopentanes
	m, CH def	*trans* CH=CCH– and *cis* CH=CH–
	C–O and C–C	**Ribose**
1013	s, p sym COC str	Ethers
	s, CH_2/CH wagging vib	Cyclopropyl compounds
	m-s, C-C vib	$-OC(CH_3)$
	vs., ring vib	Polysubstituted pyridines
—	**Tryptophan ring breathing**	—
1095	w, asym C–O–C str	Saturated aliphatic ethers, **Lipids**
	m-s, C–N str	Aliphatic amines
	s, p sym COC str	Ethers
	m-s, CCC str	Straight chain alkanes
—	**Phospodioxy group (from nucleic acids)**	—
1195	s, CH def	*cis*-(sat) CH=CH (sat)
	m-s, C–N str	Aliphatic amines
—	**Tryptophan ring breathing**	—
1276	s, CH def	*trans*-(sat) CH=CH (Sat)
	s, amide III	*trans*-secondary amides
	s, CH def	*cis*-(sat) CH=CH (sat)
1293	**s, CH def**	*trans*-(sat) CH=CH (Sat)
	m, twisting CH_2 vib	$-(CH_2)n-$
	s, amide III	*trans*-secondary amides
1315	s-m, asym N–C–N str	Ureas
	s, C–N amide III	*cis* form secondary amides
	s, CH def	*trans*-(sat) CH=CH (Sat)
—	**Guanine**	—
1395	s, amide III	Primary thioamides
	m-s, CH in-plane rocking	Aldehydes and aryl aldehydes

(Continues)

Table 2. *(Continued)*

Raman wavenumber (cm^{-1})	Type of mode	Tentative functional groups
	m-s, p sym CO_2^- str	Carboxylate ions (aq sln)
	m-s, p CH_2 def	Vinyls $-CH=CH_4$
	m-s, CH def	*cis* (sat)CH=CH(sat)
1434	m-s, CH in-plane rocking	Aldehydes
	m-s, p sym CO_2^- str	Carboxylate ions (aq sln)
	m-s, p CH_2 def	Vinyls $-CH=CH_4$
1545	s several bands ring C=C str	Benzene derivatives
—	**C6-H deformation mode**	—
1675	s, *p* C=C str	>C=C<, trans CH=CH– and isolated C=C
	s-trans form *m* C=O str	α, β unsat ketones
	s C=C str	tri and tetra alkyl alkenes and >C=C–N
—	**Cholesterol**	—
1915	*v* asym C = C = C str	Allenes
2265, 2285, 2395	*m-w*, P-H str	P–H

S, strong; p, polarized; asym, asymmetric; str, stretching; m, medium; vib, vibration; sym, symmetric; vs, very strong; def, deformation; sat, saturated; aq. sln., aqueous solution; unsat, unsaturated; w, weak; v, variable. In bold letters are indicated the main differences described in the text.

shows the PC1 *versus* the Raman wavenumber, as well as the SERS average spectra of the four mentioned fractions. Four peaks are highlighted: 780 cm^{-1}, from the P–O–P stretching related to phospholipids**;** 1075 cm^{-1}, from the C–C stretching vibration; 1315 cm^{-1}, from the CH deformation and 1745 cm^{-1}, from the C=O stretching present in phospholipids and triglycerides.[10] These characteristic peaks are in agreement with data reported by Pilarczyk *et al.*, where lipid rafts from mice aorta endothelium were studied using Raman spectroscopy and atomic force microscopy.[10] Table S1 includes additional peaks that are related to the characteristic functional groups from lipid rafts.

With these results in hand and the fact that we were able to locate the PMCA in hepatocyte DRM using biochemical techniques (Fig. 1(e)) associated with cholesterol-rich fractions and identified by SERS and PCA, we further decided to investigate the functional relationship between PMCA activity and membrane cholesterol. In particular, we were interested in how the enzymatic activity is affected when cholesterol from DRM is sequestered with MβCD. It was found that PMCA activity decreases approximately 28% when membranes are preincubated at 37 °C in the presence of MβCD-2 mM (at 2 mM MβCD, cholesterol content decreased close to 48%), an effect we are currently exploring to a larger extent. So as to expand our knowledge related to the interaction between the enzyme and membrane cholesterol, we tested the effect of cholesterol depletion at long-term incubations (24 h) employing cultured hepatocytes upon the expression of *PMCA* transcripts with real-time quantitation of the housekeeping isoforms *PMCA1* and *PMCA4*. It was confirmed that *PMCA1* is the most abundant isoform with apparent changes detected at the highest MβCD concentration directly correlated to the maximum cholesterol sequestering condition (Fig. 5(a)). While hepatocyte viability only decreased ~10% at MβCD concentrations ranging from 0.5 to 1 mM, at 2 mM MβCD viability decreased up to 60–70% compared with those of control values (Fig. 5(b)). Although the variance analysis for *PMCA1* expression in the presence of 1 mM MβCD did not show significance, this result may reflect an inflection point where a long-term response of hepatocytes to cholesterol depletion, disrupting lipid rafts, might come into view by the time cell viability starts to be compromised.

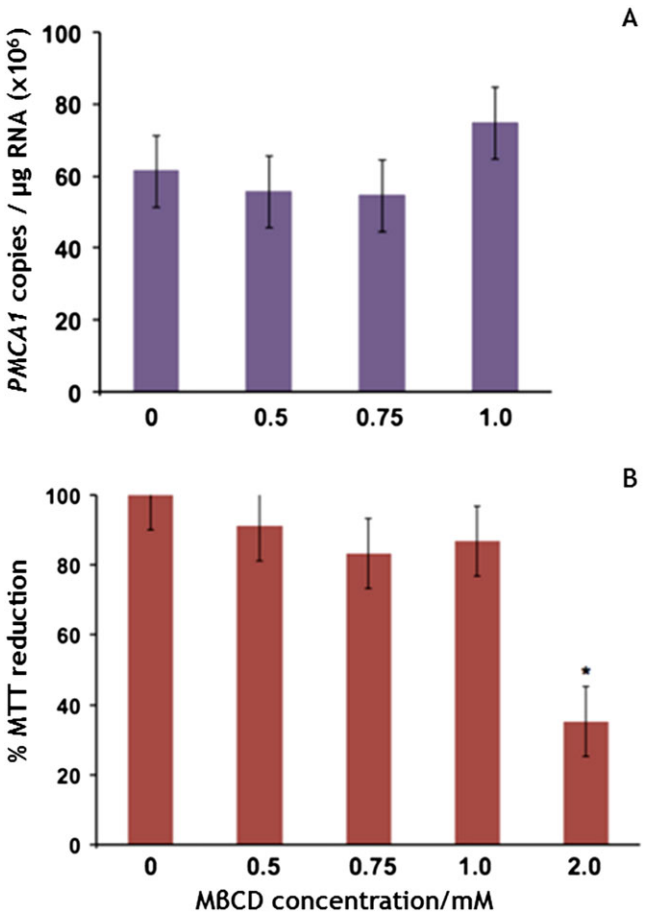

Figure 5. Effect of methyl-β-cyclodextrin (MβCD) exposure to primary hepatocyte cultures during 24 h. (a) *PMCA1* transcripts were measured by quantitative PCR (average ± SE; $n = 4$). Analysis of variance showed no significant differences between these experiments. (b) Hepatocyte cell viability was estimated by 3-(4–5-dimethylthiazol-2-yl)-2,5-diphenyl tetrazolium reduction assays ($n = 3$). Analysis of data showed statistical significance with respect to controls when 2 mM MβCD concentration was used. *$P < 0.05$ compared with control. Data were standardized as percentages to construct the plot.

Because in general the understanding of the strict mechanisms that control calcium homeostasis in cells is important to be established; for example, studying the way cells become malignant by maintaining an increased cytoplasmic calcium concentration, or as in our case, studying the way by which hepatocytes through changes in the concentration of membrane cholesterol modulate calcium translocation in direct association with pathophysiological changes in cell metabolism, the use of SERS/PCA undoubtedly represents a novel way to advance our knowledge in the study of biological membranes that eventually might help to establish the nature of these control mechanisms. Moreover, nowadays, the use of SERS/PCA is revolutionizing not only the way we track the molecular status of cells but also the methodology we use to follow altered biochemical processes caused by diseases such as atherosclerosis, fatty liver, and cancer. In the near future, this situation will undoubtedly improve diagnostics and therefore the treatment outcome for these diseases.

Conclusions

During the last few years, SERS has proven to be a robust technique with diverse applications in biomedicine, for example as a tool to detect several types of cancer and polymorphisms. To our knowledge, our study represents the first work where a DRM fraction obtained from the plasma membrane of hepatocytes has been analyzed using SERS in combination with PCA. Because the use of SERS not only confirmed fractions as cholesterol-rich domains but also allowed us to detect sphingolipid-specific signals, we consider that this method represents an excellent tool for the characterization of cell membrane fractions from different cell types. Moreover, taking into consideration that a very small quantity of sample is needed for the analysis, this technique offers important advantages that other methodologies do not provide. In relationship to the membrane distribution of PMCA and the fact that this enzyme is found associated with fractions where the protein flotillin is also found, we can suggest that PMCA is associated with lipid rafts. This finding is consistent with previous observations from our group where we described a close relationship between cholesterol and PMCA enzyme activity tightly coupled to the transport of calcium that takes place across the plasma membrane.

Acknowledgements

We thank Cristina Zorrilla-Cangas for advice on Raman microscopy, Dr José Luis González Solís for his help with PCA analysis; Javier Gallegos for literature search and Héctor Malagón for experimental animal care. This study was supported by CONACYT (Grant 180726) and DGAPA-UNAM (Grant IN-205814-3) awarded to J. M-O.

References

[1] K. Simons, K. G. van Meer, *Biochemistry* **1988**, *27*, 6197.
[2] T. Harder, K. Simons, *Curr. Opin. Cell Biol.* **1997**, *9*, 534.
[3] C. J. Fielding, P. E. Fielding, *Biochim. Biophys. Acta* **2003**, *1610*, 219.
[4] C. J. Fielding, P. E. Fielding, *Biochim. Biophys. Acta* **2000**, *1529*, 210.
[5] E. J. Smart, G. A. Graf, M. A. McNiven, W. C. Sessa, J. A. Engelman, P. E. Scherer, T. Okamoto, M. P. Lisanti, *Mol. Cell. Biol.* **1999**, *19*, 7289.
[6] A. Asanov, A. Zepeda, L. Vaca, *Biochim. Biophys. Acta* **2010**, *1801*, 147.
[7] M. T. Stockl, A. Herrmann, *Biochim. Biophys. Acta* **2010**, *1798*, 1444.
[8] J. Ando, M. Kinoshita, J. Cui, H. Yamakoshi, K. Dodo, K. Fujita, M. Sodeoka, *Proc. Natl. Acad. Sci.* **2015**, *112*, 4558.
[9] J. Cui, S. Matsuoka, M. Kinoshita, N. Matsumori, F. Sato, M. Murata, J. Ando, H. Yamaoshi, K. Dodo, M. Sodeoka, *Bioorg. Med. Chem.* **2015**, *23*, 2989.
[10] M. Pilarczyk, L. Mateuszuk, A. Rygula, M. Kepczynski, S. Chlopicki, M. Baranska, A. Kazor, *PLoS One* **2014**, *9*, e106065.
[11] S. Jin, F. Zhou, F. Katirai, P. L. Li, *Antioxid. Redox Signal.* **2011**, *15*, 1043.
[12] A. Dolganiuc, *World J. Gastroenterol.* **2011**, *17*, 2520.
[13] B. Delgado-Coello, M. A. Briones-Orta, M. Macías-Silva, J. Mas-Oliva, *Liver Int.* **2011**, *31*, 1271.
[14] D. Gebreselassie, W. D. Bowen, *Eur. J. Pharmacol.* **2004**, *493*, 19.
[15] P. A. Lanzetta, L. J. Alvarez, P. S. Reinach, O. A. Candia, *Anal. Biochem.* **1979**, *100*, 95.
[16] D. Montalván-Sorrosa, J. L. González-Solís, J. Mas-Oliva, R. Castillo, *RCS Advances* **2014**, *4*, 57329.
[17] B. Delgado-Coello, J. Bravo-Martínez, M. Sosa-Garrocho, M. A. Briones-Orta, M. Macías-Silva, J. Mas-Oliva, *Mol. Cell. Biochem.* **2010**, *344*, 117.
[18] P. J. Meier, E. S. Sztul, A. Reuben, J. L. Boyer, *J. Cell Biol.* **1984**, *98*, 991.
[19] W. H. Evans, *Biochim. Biophys. Acta* **1980**, *604*, 27.
[20] A. Mazzone, P. Tietz, J. Jefferson, R. Pagano, N. F. LaRusso, *Hepatology* **2006**, *43*, 287.
[21] J. Nagata, M. T. Guerra, C. A. Shugrue, D. A. Gomes, N. Nagata, M. H. Nathanson, *Gastroenterology* **2007**, *133*, 256.
[22] L. Jiang, D. Fernandes, N. Mehta, J. L. Bean, M. L. Michaelis, A. Zaidi, *J. Neurochem.* **2007**, *102*, 378.
[23] T. Babuke, R. Tikkanen, *Eur. J. Cell Biol.* **2007**, *86*, 525.
[24] B. Delgado-Coello, J. Santiago-García, A. Zarain-Herzberg, J. Mas-Oliva, *Mol. Cell. Biochem.* **2003**, *247*, 177.
[25] B. Delgado-Coello, R. Trejo, J. Mas-Oliva, *Mol. Cell. Biochem.* **2006**, *285*, 1.
[26] F. Kessler, O. Bennardini, O. Bachs, J. Serratosa, P. James, A. J. Caride, P. Gazotti, J. T. Penniston, E. Carafoli, *J. Biol. Chem.* **1990**, *265*, 16012.
[27] T. P. Stauffer, H. Hilfiker, E. Carafoli, E. E. Strehler, *J. Biol. Chem.* **1993**, *268*, 25993.
[28] E. C. Le Ru, E. J. Blackie, M. Meyer, P. G. Etchegoin, *J. Phys. Chem. C* **2007**, *111*, 13794.
[29] J. R. Beattie, S. E. J. Bell, B. W. Moss, *Lipids* **2004**, *39*, 407.
[30] C. Krafft, L. Neudert, T. Simat, R. Salzer, *Spectrochimica Acta Part A* **2005**, *61*, 1529.
[31] H. Wu, J. V. Volponi, A. E. Oliver, A. N. Parikh, B. A. Simmons, S. Singh, *Proc. Natl. Acad. Sci.* **2011**, *108*, 3809.
[32] A. C. S. Talari, Z. Movasaghi, S. Rehman, I. U. Rehman, *Appl Spectros Rev* **2015**, *50*, 46.
[33] S. W. Fogarty, I. I. Patel, F. L. Martin, N. J. Fullwood, *PLoS One* **2014**, *9*, e106283.

Supporting information

Additional Supporting Information may be found online in the supporting information tab for this article.